

An Active Stereometric Triangulation Technique Using a Continuous Colour Pattern

A. Knoll¹ and R. Sasse²

¹ Bielefeld University, Faculty of Technology, Postfach 10 01 31, D-33501 Bielefeld

² Technical University of Berlin, Computer Science Department, Sekr. FR 2-2,
Franklinstr. 28, D-10587 Berlin

1 Overview

We present a novel method for obtaining dense range maps, which is based on the combination of two (or more) colour cameras and the projection of a continuous colour pattern. The technique offers several advantages for use in robotics including the potential for very high speed of operation and for higher accuracy than achievable with other active triangulation techniques that employ discrete coloured light stripes or sequential binary-encoded monochrome patterns. The high speed enables the range image generation of fast moving objects in highly dynamic environments. In this approach a continuous colour pattern with uniform brightness is projected onto the objects in the scene.

The objects so illuminated are seen by the two cameras. Corresponding points in both images are then searched for in a manner similar to passive stereo. The criterion to be met by correspondences is that they have the same (relative) colour in both images. Knowledge or recognition of the absolute colours (which were emitted by the projector) is therefore never needed; this makes the method insensitive to colour changes caused by the object and prevents false matches at object discontinuities. Moreover, the method is quite insensitive to geometric distortions and reflectance variations. A working prototype system based on this principle has been realised using standard low cost optical components. Our findings indicate that distance resolutions on the order of 1% of the measured distance are easily achievable. It was shown experimentally that this is true for most materials with different reflectance functions used for technical products (metals, all kinds of plastics, foams).

1.1 Problem Definition

Active triangulation techniques for measuring distances or for generating range images have been in widespread use in the computer vision and robotics research community for a long time [Altschuler 79, Boissonat 81]. Successful applications in in-

dustry have also been reported, e.g. [Pritschow 91]. Various designs with different numbers of cameras and lighting patterns are conceivable to match the most diverse range of applications (see [Vuylsteke 90] for an overview and [Sasse 93] for further introductory notes). Besides this flexibility, the advantages of all of these methods include the potential for high measurement accuracy and resolution, independent of the ambient lighting conditions. The common disadvantage of these methods are their limited distance range and, if they are used to generate dense depth maps, their slowness. While the former disadvantage is a direct consequence of the need for active lighting and can be removed when the target application is known, the latter results from the use of mechanical scanners, which direct the lighting pattern over the scene.

This problem of slow data acquisition can be overcome by projecting lighting patterns consisting of many elements, e.g. a multitude of points or lines, and thereby illuminating more points or areas of the scene. As the number of simultaneously illuminated areas increases, their spatial distance on the object surface decreases and it is no longer possible to recognise the elements of the pattern individually. Moreover, the spatial order of the elements seen by the camera does not necessarily correspond to the order which was projected. The resulting danger of misinterpretation, particularly at object discontinuities, gives rise to the need of *coding* the pattern elements in a unique manner. Coding can refer to time (by sequentially projecting a series of different patterns on the scene), to structure (by projecting a pattern consisting of individually recognisable elements of different brightness or shape), to frequency (by projecting a colour pattern), or any combination of the three.

Probably the most well known of the time-sequential methods is binary encoded structured light [Altschuler 79, Gutsche 91]. In this approach a series of patterns masks is projected, each of which consists of a different spatial sequence of alternating black and white stripes. Thus, every point on the object receives a different time-sequence of black and white intensity values, which marks it unambiguously for identification. If a sequence of n pattern masks is used, this corresponds to $2^n - 1$ projected stripes. The problems with the method are the exact alignment of the stripes in all masks and the need for objects that do not move while the n images are recorded. The former problem has been alleviated by the advent of LCD-shutters used in recent designs (which need about one second to record 8 projections), but the difficulties arising from the need for taking n pictures remain. However, since every line must have a minimal spatial extent, the resolution of the range image is limited.

These difficulties can be eliminated if a binary pattern is constructed in such a way that a great number of arrays are projected, each containing, for example, 3×3 dots. The distribution of black and white dots within each array is different from the constellation in all other arrays. Thus, if an appropriate coding scheme with a large Hamming-distance is used, a great number of areas can be marked unambiguously in the scene. A sophisticated implementation of this structure-based approach is described in [Vuylsteke 90b]. Here, the resolution of the range image is also limited because every block must have a minimal spatial extent. Moreover, problems exist with surfaces that exhibit strong textures.

1.2 Advantages of the Approach

With the method described in this paper, a special *continuous* non-repetitive pattern of hues illuminates the entire scene. The object so illuminated is seen by two colour-cameras. Correspondences of all points visible in both cameras can be found from a single pair of images. The search process is similar to the process employed with passive stereo. This obviates the need for scanning and makes the generation of dense range images from a single snap-shot possible. Thus, the acquisition time is only dependent on the shutter speed of the cameras. This is in contrast to all serial triangulation techniques and enables the range image generation of fast moving objects. Consequently, a sensor based on the technique is immune to motion problems.

Since two cameras in a stereoscopic configuration are used, the criterion to be met by corresponding points is that they have the same colour in *both* images. This colour is not necessarily equivalent to the colour that was emitted from the light source. This is the reason, therefore, that the method is perfectly well suited to non-structured scenes of uniform intensity (a search for edges or prominent object features is never necessary) but sets it apart from other colour-based techniques that employ a sequence of colour stripes whose absolute colour must be identified in an image recorded with a single camera [Boyer 87, Plaßmann 91, Monks 92]. Unlike these, the proposed method is insensitive to colour changes caused by the object (provided they evenly affect both cameras) and does not depend on special cameras with high response stability over a large dynamic range (such as the method described in [Tajima 87]). Preliminary findings (see sec. 3) indicate that this is true for most materials with different reflectance functions, which are used for technical products (metals, all kinds of plastics, foams). Moreover, this point-based method does not depend on the identification of object features. Once the correspondence search is accomplished, the distance of the image points can be calculated by simple triangulation. This implies that the accuracy of the method is only limited by the ability of the cameras to differentiate between colours and their spatial resolution. There is no principal lower limit to accuracy inherent to all methods relying on discrete patterns. The experiments undertaken with inexpensive single-CCD colour cameras show an accuracy that is slightly lower than achievable with a scanned laser light sheet and the same recording hardware. It is, however, more than sufficient for assembly operations and was obtained without any pre-processing of the data. On average, about 70% of all points in the image were matched.

Furthermore, due to the recording of the scene with two cameras, the position and the orientation of the light source are irrelevant; this minimises the amount of calibration required before measurements can be taken. Other than for the cameras, there is no calibration necessary. In particular, this makes it possible to move the cameras (mounted, for example, on a robot end effector) between the measurements with the projector remaining in place. Lastly, the areas (if any) on the object where no results can be obtained (e.g. due to occlusions) can be identified easily from the measured data. Assignments of non-corresponding points in the two images or,

conversely, missing assignments of corresponding points, i.e. false matches such as familiar from passive stereo, are unlikely.

2 The Principle of Operation

The basic principle of operation is depicted in fig. 1.1: The projector illuminates the scene (of which only a single arbitrary object point O is shown in the figure) with the colour pattern.

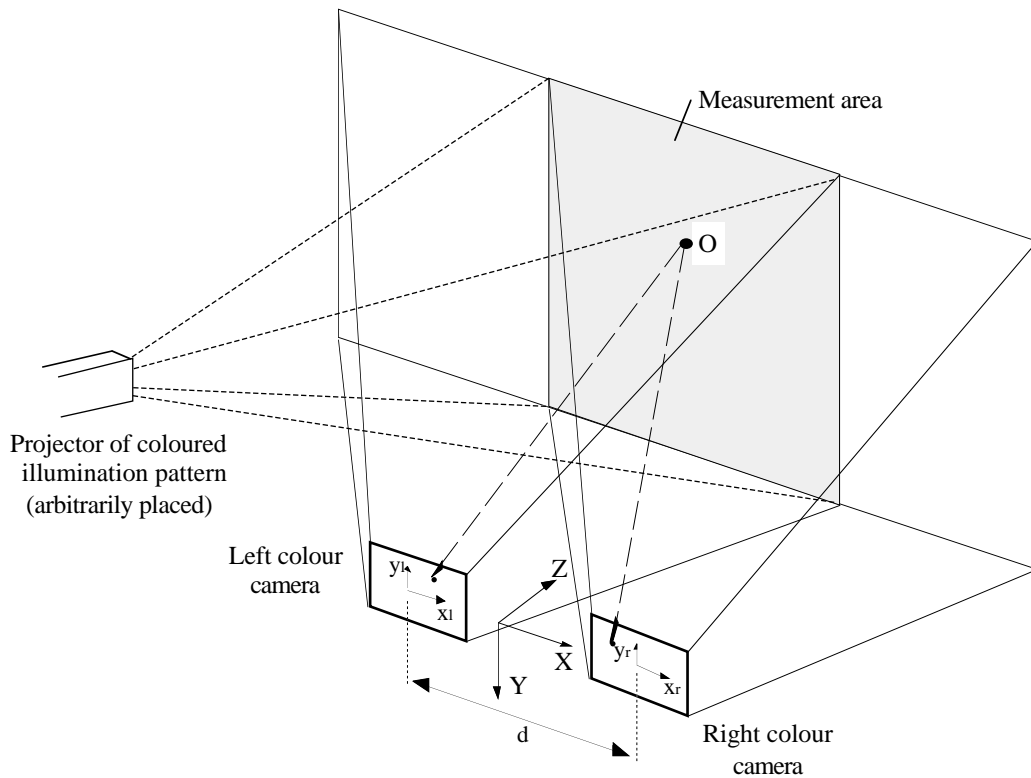


Fig. 1.1 This shows the basic set-up for implementing the method.

In fig. 1 the measurement area is the intersection of the viewing areas of the two colour cameras and the area illuminated by the projector. The coordinate system (X, Y, Z) is the world system; d is the baseline of the cameras. The systems (x_l, y_l) and (x_r, y_r) are the internal camera coordinate systems. The pattern consists of a multitude of colour hues in the horizontal direction, in the vertical direction the individual colour does not change. In other words: the colour values change only in one dimension, i.e. they vary continuously as we move over the projection plane from left to right (X -direction in fig. 1) but remain constant when we move vertically (in the Y -direction). Thus, from the projector's point of view, every vertical

line (ideally an infinitesimally small stripe) of the object is marked with a unique colour. All of these coloured object lines are seen by the left and right camera. Depending on the object geometry, reflectance and colour these lines are, however, distorted (or even interrupted) and the colour that is recorded may no longer be the colour that was projected. While the distortion of the lines is the basis for calculating the distance Z of objects points by all triangulation techniques, the object-induced shifts in colour are an unwanted, yet inevitable, effect encountered in all practically relevant scenes. For a detailed analysis of the dichromatic colour reflectance model justifying the methods of both the correspondence search and the colour correction outlined below we refer the reader to [Klinker 90, Sasse 93].

Since the goal is to identify an individual object point by the colour received from it, the criterion for the correspondence search is the value of the received colour, no matter how it compares with the projected colour. Nevertheless, since the correspondence search relies on the comparison of the colours in both cameras, it is necessary that the colour shift due to the object colour result in the same colour in both cameras. In the course of our experiments we have found that this precondition is met in most cases, whereas in accordance with the dichromatic reflection model the absolute colours frequently change dramatically between projection and recording (this precludes the use of single-camera techniques as described in [Tajima 87], which recover colour-stripes on the object from the knowledge of the exact position of the projected hues).

Other than for the fact that the projector must be able to project a colour pattern and the cameras must record colour images, there is no essential difference from standard stereo setups. This makes it particularly easy to fuse the results obtained from (colour) images recorded with ambient lighting (passive stereo) and the results from the active coding technique. We shall now detail the possible colour patterns and subsequently describe the correspondence search.

2.1 The colour pattern

There is an unlimited number of colour coding patterns conceivable, all of which can be specified by defining the intensity distribution functions of the three colour components (e.g. red-green-blue, RGB) over the projection plane. Depending upon the application one can think of colour-sequences obtained from varying the three colour components according to a simple function (e.g. three phase-shifted sine-functions of the same spatial frequency) or a system of orthogonal functions (e.g. Walsh-functions of different frequencies) as most appropriate for constructing the pattern. Although a full discussion would go beyond the scope of this paper, we would like to mention that it is not necessary to restrict the pattern to structures that vary only in one dimension, i.e. in the X -direction in fig. 1. One can also think of patterns whose colour component intensities follow superposed two-dimensional spatial wave-fields of colour patches with random colour, random structure, or both and of coloured pseudo noise sequences similar to the coding pattern in [Vuylsteke

90]. Random patterns hold some promise for scenes with completely unknown object structures, but have not yet been examined in this context.

No matter what structure seems most appropriate for a given application, the pattern should be so designed as to facilitate the correspondence search process even in the case of a low signal-to-noise ratio by providing additional hints about the most likely colour value of the object point under consideration (see below). Making use of such redundancies or a priori knowledge can obviously increase the “hit rate” of the search process and speed it up considerably. Although we feel that the exploration of the advantages and disadvantages of different classes of patterns hold much promise for the future, we have restricted ourselves to the class of line patterns, i.e. patterns whose colour changes only in one dimension (as outlined above).

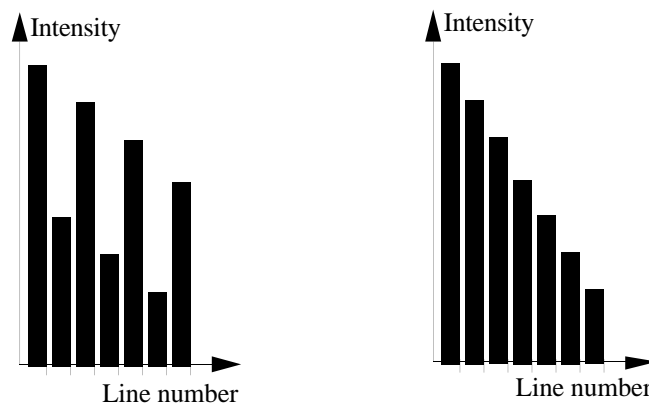


Fig. 2.1 High contrast (left) and low contrast (right) illumination. Both diagrams show the intensity of one colour channel (e.g. red) for seven consecutive lines of the colour pattern.

In principle, these patterns fall into two categories: High contrast and low contrast line sequences (see fig. 2.1). With high contrast sequences the colour changes rapidly from line to line (and returns almost to the original value one or two lines later) whereas with low contrast illumination the colour changes smoothly over the whole pattern plane. In the first case the individual lines may easily be differentiated between on smooth surfaces while at object discontinuities (e.g. edges, corners or object boundaries) the contrast may become very low. Obviously the reverse is true for low contrast illumination with a continuous change in colour: Here, the distinction between the lines may be more difficult on smooth surfaces but an object discontinuity will always produce a high colour contrast in the image. It should be pointed out that the width of the lines is one of the limiting factors of the distance resolution and must therefore be chosen very carefully.

In practice the high contrast approach yields acceptable results only if the image of every line is projected on exactly one pixel column of the image plane of the camera. For general geometries and with a fixed pattern this requirement can only be met for a fixed distance. Otherwise, adjacent lines are mapped to one pixel or, on the contrary, one line is mapped to several pixels. In either case of misalignment the contrast in the image is lost. Moreover, if an ordinary light projector with a small

depth of focus is used, a satisfactorily sharp image of the colour pattern can be projected only within a small range of depth. As the scene object moves too close or too far away from the projector, the pattern becomes blurred, which also reduces the contrast. Obviously, this problem also occurs when low contrast illumination is used, but the deterioration in resolution is much less severe.

In order to make maximum use of the ability of the camera to distinguish between colours, the pattern should have the highest possible colour range, i.e. it should consist of all the colours the camera can recognise. In other words: from the left to the right end of the projection plane the entire visible spectrum should be run through.

2.2 Colour Correction, Noise Elimination and the Search for Correspondences

If the intensity response of the cameras were uniform over the entire frequency spectrum, arbitrary patterns would be reproduced without distortion. However, inexpensive single-chip CCD cameras, such as used in our experiments, frequently exhibit a much lower sensitivity to blue than to red and green hues. It is therefore mandatory to equalise the outputs of the colour channels of both cameras before searching for corresponding points. This process will be referred to as *colour correction*.

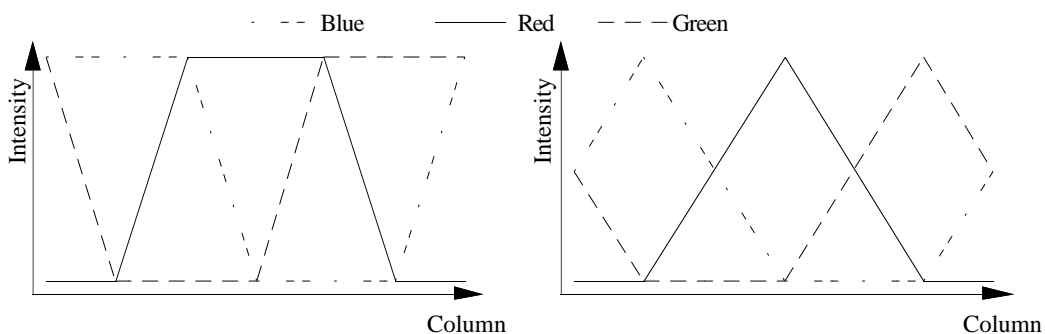


Fig. 2.2 These are compositions of the colours for low contrast sequences. Left: At any pixel one of the three colour components equals zero. Right: In addition to one component being zero, the intensity of the pattern is uniform.

There are two other main difficulties related to the cameras: Perspective distortion and the superposition of random observation noise generated in semiconductor recording devices. While perspective distortions can be sufficiently reduced by applying standard camera calibration techniques, observation noise becomes a severe problem when areas in the image are examined in which one or more colour channels produced a low signal (superposed by a more or less constant noise level), i.e. in areas of a low signal-to-noise-ratio. An elegant way of circumventing this problem is the exploitation of redundancy or additional a-priori information built into the pattern, e.g. by restricting the full choice of colours or by letting colour values rise and fall over the projection plane in a well-defined manner. We now look at two

possible patterns which contain information enabling both noise suppression and colour correction.

The values of the three basic colours of these special patterns as a function of the pixel column are shown in fig. 2.2. With both patterns, at any image column either of the three colour components is zero while the other two are anywhere between zero and their maximum intensity. For the purpose of *noise suppression* the weakest component in the image can therefore be set to zero in the vicinity of the object point even if the recorded image due to noise effects suggests the contrary. More formally:

$$I(j;x) := \begin{cases} 0 & \text{if } I(j;x) = \min[I(R;x), I(G;x), I(B;x)] \\ I(j;x) & \text{otherwise} \end{cases}$$

where $I(j;x)$ is the intensity of an image point, $j \in \{R, G, B\}$ and x is the column number of the image line under consideration. This is obviously a very simple, nevertheless quite useful strategy. More elaborate schemes may employ redundancy checks, such as familiar from coding theory, or matched filters.

In the experiments colour compositions according to the second function shown in fig. 3 were used. Not only is either of the three components zero, in addition the intensity (brightness) of the resulting projected pattern is uniform over the entire plane. This enables the application of very simple scaling operations to the recorded image: After setting the smallest colour component to zero, the two remaining components are multiplied by a common factor. This factor is so chosen as to make the sum of the two match the required brightness, i.e.:

$$I(j;x) := \lambda \frac{I(j;x)}{I(R;x) + I(G;x) + I(B;x)}$$

where λ is the maximum intensity value of a colour channel, which equals the (uniform) sum of all three components R, G and B. For an eight bit quantizer, $\lambda = 255$. Although the following step of *correspondence search* relies only on the relations between the colours at (or around) the pixel under consideration, the scaling, which does not alter these relations helps to simplify the search procedure.

We conclude this section by briefly introducing the procedure of correspondence search which we found most useful in the experiments (although much more complicated colour metrics are conceivable, they do not necessarily justify their increased complexity by the obtained results). Our pragmatic approach is centred around an intensity based comparison of colour value relations over the two epipolar lines of the left and right image (with the appropriate local and global disparity limits). Since due to different observation angles the intensity of the colours in the two images may be different, the basic idea underlying the procedure is that the colour reflected off a certain pixel is determined mainly by the largest of the three colour components. We assume that the colour vectors at an arbitrary pixel in the left and right image are linearly dependent, i.e. they are multiples of each other:

$$\begin{pmatrix} R_l \\ G_l \\ B_l \end{pmatrix} = s \begin{pmatrix} R_r \\ G_r \\ B_r \end{pmatrix}$$

In order to scale the two colour vectors before applying the similarity measure, the factor is determined as follows:

```

m := max(Rl, Gl, Bl)
IF      m = Rl THEN s := Rl / Rr
ELSFIF m = Gl THEN s := Gl / Gr
ELSE           s := Bl / Br
END

```

Subsequently, do determine the similarity between two pixels to be compared at column positions x_l and x_r , the squared vector distance between the two individually scaled vectors of all correspondence candidates is computed according to:

$$Q(x_l, x_r) = \sum_{i=-N}^N \left[\left(R_l(x_l + i) - s_i R_r(x_r + i) \right)^2 + \left(G_l(x_l + i) - s_i G_r(x_r + i) \right)^2 + \left(B_l(x_l + i) - s_i B_r(x_r + i) \right)^2 \right]$$

where i runs over a window of size $2N+1$ (two-dimensional windows are also possible, but at the expense of higher algorithmic complexity). The candidate for which $Q(x_l, x_r)$ reaches a global minimum within the considered image line is chosen as the corresponding point (for x_l).

The reader is referred to [Sasse 93] for further details on colour models, colour correction, noise elimination, image smoothing, correspondence search and colour interpolation for imaging setups with converging optical axes, i.e. for geometries with epipolar lines not corresponding to pixel lines or columns. In the following section practical issues will be examined and measurement results will be presented.

3 Implementation and Experimental Results

A large number of different scenes with different objects were evaluated using a simple experimental setup with two single-chip colour CCD cameras. Their resolution was 512×512 pixels, their focal length $f = 8\text{mm}$, the base width was $d = 200\text{mm}$. The angle of convergence (the angle the optical axis of the camera makes with the imaginary optical axis of a setup for parallel line stereo) was 15° .

To illustrate the quality of the image data produced by our setup, fig. 3.1 shows the output of the three colour channels when the camera sees a uniform white

reflector illuminated by a pattern according to fig. 2.2 (right). The colour correction algorithm was already applied to the output, equalising severe slowly varying changes in the intensity amplitudes (resulting in peaks of different heights).

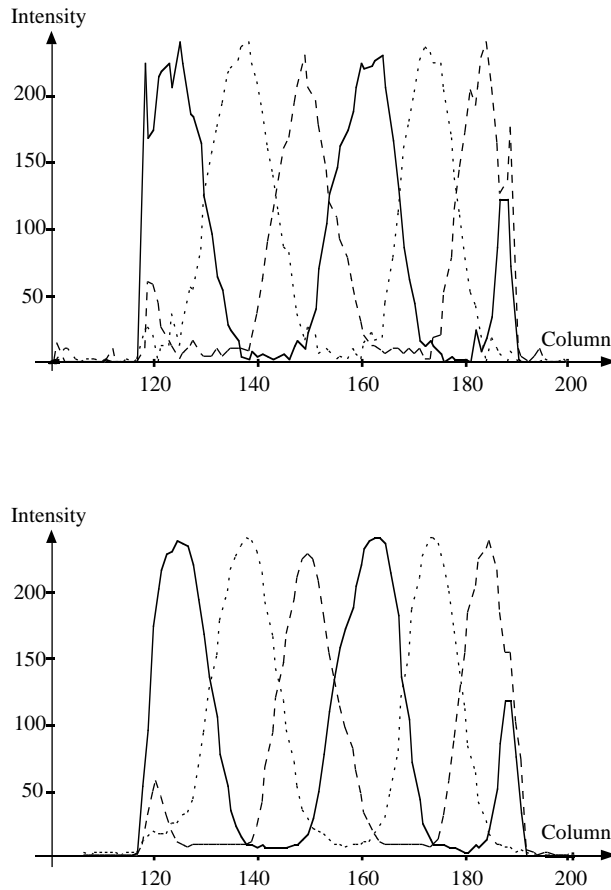


Fig. 3.1 Real intensity data of the three colour channels along one image line produced from a test scene. Top: Intensity after colour correction (scaling). Bottom: Result after application of a smoothing operator.

The remaining disturbances were removed (fig. 3.1, bottom) by a smoothing operator on the colour-corrected data. This obviously leads to somewhat “blurred” intensity data and thus limits the local spatial resolution of the distance measurement. It speaks for the robustness of the approach that the distance measurements are of a more than acceptable accuracy despite the low quality of the acquired data.

An analysis of the geometrical arrangement of our setup [Ottink 89] yields a principal distance error of about 2mm over a distance range of $z = 100 \dots 550$ mm. This accuracy can be obtained only if the correspondence search is error-free, which in turn presupposes cameras of higher quality than we could afford. Nonetheless, using only the comparatively simple relations given in the previous section, an absolute error in distance of better than 1% of the measured distance was achieved.

The number of pixels for which the correct distance was computed was on average 75%. Note that this holds despite the low quality of the input data.

Table 3.1 Absolute distance errors for white reflector

Distance Z [mm]	Error ΔZ [mm]
250	1,5
300	2,3
350	2,0
400	1,9
450	3,0
500	2,6
550	4,0

Table 3.2 Absolute distance errors for different reflectors, $Z=350$ mm

Material	Error ΔZ [mm]
White Cardboard	1,46
Wood	1,67
Plastics, bright	1,72
Steel	2,80
Aluminium	2,80
Plastics, dark	3,74
Brass, polished	3,84

Table 1 lists the mean absolute distance error for different distances. The values were obtained by evaluating several hundred measurements of a known distance Z . In table 2 the absolute error is given for different materials of the reflector. These values were recorded to justify our claim of the method working independently of the reflectance properties of the reflector. Note that the error increases as the reflection grows. Note further, however, that the value for polished brass was obtained although a human observer due to the optical properties, which much resemble that of a mirror, would only see specular reflections, if anything.

To increase the precision of the measurements further, the distance may be computed with sub-pixel accuracy. This was not done to obtain the readings listed in tables 1 and 2, but is straightforward to implement: upon completion of the search process, the position of the corresponding point and the position of that of the two neighbours on the epipolar line which has the lower value of the similarity function Q are interpolated. The weights of the interpolation are the two values of Q for the corresponding point and its neighbour.

In the remaining part of this section we present two examples of range maps obtained from real world objects and in a real world environment. The ambient lighting conditions were those of a normal office room with the brightness changing continuously. The objects which were not used for calibration purposes were all taken from real assembly processes and not modified.

To illustrate the method's insensitivity to varying reflection due to oblique surfaces, in the first example an object with a triangular surface was measured. The object was so positioned as to avoid occluding contours. For evaluation a rectangular area was selected in the recorded images, which was completely illuminated with the pattern. Within this area the correspondences were determined using the procedure outlined above. The range map produced with the distances computed based on these correspondences is shown in fig. 3.2.

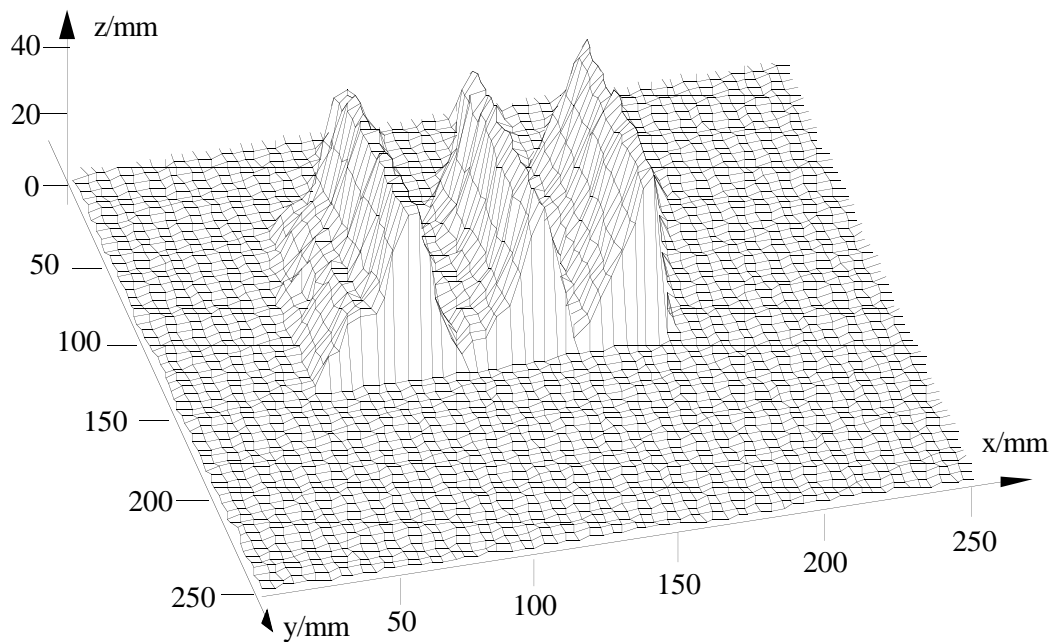


Fig. 3.2 Three dimensional plot of the range map obtained from the object mentioned in the text. All distances are given in mm. The maximum error is about 2mm over the entire area.

The second example is much more complex. It contains all the difficulties one is faced with when measuring distances with either active or passive stereo vision systems. The object (fig. 3.3) has a uniform diffuse surface, it has smooth curvatures as well as sharp edges, it produces shadows and has occluding contours. Lastly, in spite of the diffuse surface, it generates specular reflections.

Fig. 3.4 shows the digitised recorded image of the left camera before colour correction. It shows quite well the irregular distribution of the colour intensities due both to the locally different frequency response of the camera and to the geometrical distortions introduced by the pattern projector. This effect is well visible at the left upper transition from green to red. Points of equal intensity are mapped to ovals instead of parallel vertical lines.

Fig. 3.5 shows the range map of the object in fig. 3.3. Due to the high density of points for which distances were obtained, a three dimensional black-and-white plot was inadequate. Instead, a false colour picture was produced with the colours representing the distances. The scale bar on the left side indicates the distance: It is purple at its lower end and orange at its upper end. This change in colour corresponds to a linear change in distance between $Z = 230$ mm and $Z = 310$ mm. A black dot represents a pixel of unknown distance, i.e. an image point for which no corresponding point was found (positive false match). All the points displayed in the range map were extracted from the original image data (fig. 3.4) during the initial search, no interpolation or iterative search was performed to provide values for the points that were not assigned a distance after this first step. A window size of 9 pixels was used for correspondence search, the global disparity limit was the interval $[230\text{mm}, 310\text{mm}]$, the number of pixels under investigation was 102960, of which 73375 were found after 2 hours of computation on a VAXstation.

<The following three colour images can be found in a separate PostScript file>

Fig. 3.3 View of the object used in the second example.

Fig. 3.4 Object as seen by one camera.

Fig. 3.5 Range map obtained for the object. See text for explanations.

There are about 10% of negative false matches, of which about 75% are in the area of the particularly weak blue channel. This means that for this particularly difficult object about 71% of the pixels were assigned the correct distance (with an absolute error of much less than 1mm), 10% a more or less deviating distance and the rest of 19% no distance. It is obvious that even simple iterative strategies like hierarchical search or hypothesis-test procedures may considerably improve these figures in an environment of a false match. However, even without such more elaborate schemes, a hit rate of 71% is acceptable given in particular the shortcomings of the physical setup. A further discussion of the residual errors and the remaining problems can be found in [Sasse 93].

4 Conclusions

We have presented a fast and accurate method for generating range images of objects of arbitrary shape and surface. Its potential reaches far beyond the standard applications of active stereo vision. Since there is no principal lower physical limit of its size, it can be miniaturised using fiber optics for providing the necessary light at the point of measurement or for picking up the images, or both. This would enable the method to be employed for measuring the environment of small artificial anthropomorphic hands. Moreover, since only standard hardware is used, the method lends itself to the combination with passive (colour) stereo, such a combination would bring together the advantages of both approaches without trading in their deficiencies.

As far as the improvement of the accuracy and of the hit rate are concerned, the following lines of research can easily be identified:

- Modelling and compensation of the non-linearities of the cameras, parameterisation to account for differences between left and right camera.
- Extension of the camera calibration, which should take non-linear errors into account.
- Different coding of the pattern to improve the redundancy and to increase the signal-to-noise ratio and the contrast between two columns of the pattern. This would allow the filtering algorithms to be adapted and to exploit this a priori knowledge.

- Inclusion of subpixel techniques.
- Improvement and miniaturisation of the pattern source.
- Development of appropriate processor architectures to obtain video-frequency generation of range maps.

Even without a realisation of these advanced topics, the method can be utilised for solving easily several of the problems encountered whenever computer vision systems are intended to help perform recognition tasks on the factory floor.

5 References

- Altschuler 79 Altschuler, M., Altschuler, B., Taboada, J.
Measuring Surfaces Space-Coded by a Laser-Projected Dot Matrix
Proc. SPIE, Vol. 182, 1979
- Boissonat 81 Boissonat, J., Germain, F.
A new Approach to the Problem of Acquiring Randomly Oriented Workpieces out of a Bin
Proc. 7th Int. Conf. on Art. Intell., IJCAI-81, 1981
- Boyer 87 Boyer, K., Kak, A.
Color-Encoded Structured Light for Rapid Active Ranging
IEEE Trans. on Pat. Anal. and Mach. Intell., Vol. PAMI-9, No. 1, Jan. 1987
- Gutsche 91 Gutsche, R., Stahs, T., Wahl, F.
Path Generation with a Universal 3d Sensor
Proc. 1991 IEEE Conf. on Robotics and Autom.
- Klinker 90 Klinker, G. J., Shafer, A., Kanade, T.
A Physical Approach to Color Image Understanding
International Journal of Computer Vision, Nr. 4 (1990), pp. 7-38
- Ottink 89 Ottink, F.
Kalibrierung eines Roboter-Kamera-Systems
Studienarbeit, Institut für Techn. Informatik der TU Berlin, 1989.
- Ottink 90 Ottink, F.
Grundlagenuntersuchung zur Laserstereoskopie
Diplomarbeit, Institut für Techn. Informatik der TU Berlin, 1990.
- Pläßmann 91 Pläßmann, P.
Measuring the Area and Volume of Human Leg Ulcers Using Colour Coded Triangulation
Proc. 1. Conf. on Advances in Wound Management, Cardiff, 1991
- Pritschow 91 Pritschow, G., Horn, A.
Schnelle adaptive Signalverarbeitung für Lichtschnittsensoren
Robotersysteme, No. 4, 1991, Berlin: Springer-Verlag
- Sasse 93 Sasse, R.
Bestimmung von Entfernungsbildern durch aktive stereoskopische Verfahren
Dissertation, TU Berlin, Fachbereich Informatik, 1993
- Tajima 87 Tajima, J.
Rainbow range finder principle for range data acquisition
Proc. IEEE Workshop Ind. Appl. of Mach. Vision and Mach. Intell., Feb. 1987
- Vuylsteke 90 Vuylsteke, P., Price, C., Oosterlinck, A.
Image Sensors for Real-Time 3D Acquisition
ASI Series F, Vol. 63: Traditional and Non-Traditional Robotic Sensors, Berlin: Springer-Verlag, 1990
- Vuylsteke 90b Vuylsteke, P., Oosterlinck, A.
Range Image Acquisition with a Single Binary-Encoded Light Pattern
IEEE Trans. on Pat. Anal. and Mach. Intell., Vol. PAMI-12, Feb. 1990

